

Hill's and Huxley's Muscle Models – Tools for Simulations in Biomechanics

Kosta Jovanović¹, Jovana Vranić², Nadica Miljković³

Abstract: Numerous mathematical models of human skeletal muscles have been developed. However, none of them is adopted as a general one and each of them is suggested for some specific purpose. This topic is essential in humanoid robotics, since we firstly need to understand how human moves and acts in order to exploit human movement patterns in robotics and design human like actuators. Simulations in biomechanics are intensively used in research of locomotion, safe human-robot interaction, development of novel robotic actuators, biologically inspired control algorithms, etc. This paper presents two widely adopted muscle models (Hill's and Huxley's model), elaborates their features and demonstrates trade-off between their accuracy and efficiency of computer simulations. The simulation setup contains mathematical representation of passive muscle structures as well as mathematical model of an elastic tendon as a series elastic actuation element. Advanced robot control techniques point out energy consumption as one of the key issues. Therefore, energy store and release mechanism in elastic elements in both tendon and muscle, based on the simulation models, are considered.

Keywords: Biomechanics, Musculoskeletal Modeling, Computer Simulation, Energy Distribution.

1 Introduction

This paper presents a part of the current research at the School of Electrical Engineering in Belgrade in the field of exploiting bio-inspired solutions in technical world and particularly in robotics. Knowing that future service robots will be most likely humanoids that can easily fit within our environment fully accommodated for humans, we need to have extensive insight and comprehensive understanding of human anatomy, physiology and human control patterns. To that end, we need accurate mathematical models which

¹ETF Robotics Laboratory, School of Electrical Engineering, University of Belgrade, Bulevar kralja Aleksandra 73, 11000 Belgrade, Serbia; E-mail: kostaj@etf.bg.ac.rs

²Friedrich-Alexander Universität Erlangen-Nürnberg, 91054 Erlangen, Germany;
E-mail: jovanavranic@gmail.com

³BioMedical Instrumentation & Technologies Laboratory, School of Electrical Engineering, University of Belgrade, Bulevar kralja Aleksandra 73, 11020 Belgrade, Serbia and with Tecnalía Serbia Ltd., 13/6 Vladetina, 11000 Belgrade, Serbia; E-mail: nadica.miljkovic@etf.bg.ac.rs

would accurately represent real biological systems and assist our understanding and studying them. In [1], we suggested the technical paragon to the antagonistic human actuation system, while in [2] we pointed out necessity of accurate mathematical model in robot design and control with the final aim to enable safe human robot interaction. There have been numerous attempts to create artificial muscles (Fig. 1) and therefore exploit advantages of muscles as main movers: pneumatic McKibben pneumatic actuator [3], piezoelectric muscle-like actuator [4], electroactive polymer actuators as artificial muscles [5], shape memory alloys [6], and other solutions. However, they all require good understanding of human muscle physiology and patterns of muscle behaviour, in order to inherit principles of the biological solution. This study presents different mathematical models of human muscles as the most advanced actuators, whose power-to-weight ratio is far superior to all conventional actuators so far [7].

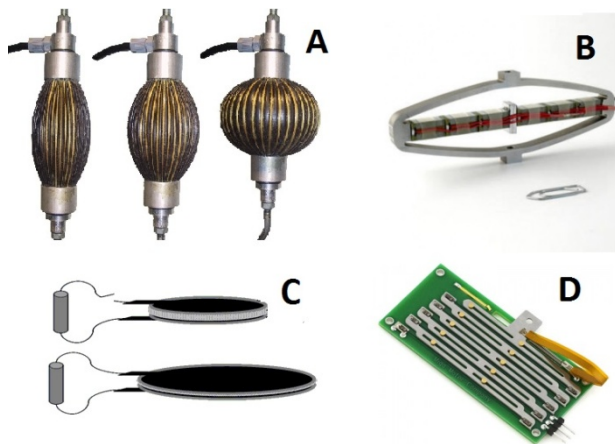


Fig. 1 – *Artificial muscles: A-McKibben pneumatic actuator, B-piezoelectric muscle-like actuator, C-electroactive polymer actuators, D-shape memory alloys.*

In this study we outline Hill's and Huxley's muscle models [8, 9], compare them and conduct comparative analysis by computer simulations. We elaborated advantages of both models, necessary extensions by numerical simulations, and point out the possible use of the models through the simulation experiments. Some typical patterns of human muscle activity are used to make comparison among the models and prove the validity by comparing to the real muscle behaviour. Relations between force, length and velocity of the skeletal muscle, in addition to muscles and bone topology are of major importance for resulting dynamic impedance behaviour in contact tasks for humans. Therefore, this study will assist in analysis of energy efficiency of human muscle pairing,

voluntary control of compliance in contact tasks, and optimization analysis of the human musculo-skeletal system.

Numerous authors have already presented technical realization of human-like actuation in cutting edge robotics. At Osaka University antagonistically coupled pneumatic actuator is described in [10]. In German Aerospace Center (DLR) tendon driven antagonistic robotic actuator is demonstrated in [11]. Japanese robot Kenshiro from University of Tokyo [12] and ECCEROBOT designed by the European consortium [13] are prime examples of robots that fully exploit a musculo-skeletal human structure and therefore highlight importance of the research presented in this paper.

Section 2 of the paper gives short overview of muscle physiology, Section 3 presents common muscle structures and the two corresponding models. In Section 4 simulation results and correlation level between mathematical models to real muscles behaviour are presented. Section 5 demonstrates model based analysis of energy distribution between elastic properties within a muscle and its tendon. Finally, some remarks are made and tips for future work are stated in the Discussion and Conclusion Section.

2 Review of Muscle Physiology

There are three types of muscles: skeletal, heart, and smooth muscles. Skeletal muscles make up a major part of the body. Heart muscle is striated like skeletal muscle, but is never tetanized in its normal function. Instead, it functions in single twitches, which are evoked by electrical impulses from Sinus-Atrial node (SA) node. Smooth muscles are not striated, and are not controlled voluntarily. The examples for this kind are muscles that surround blood vessels or linings of organs.

The focus in this paper is on skeletal muscles since they are involved in movements such as locomotion. Skeletal muscles are controlled by the nerves. When neural impulse reaches muscle tissue it causes the muscle contraction and during the contraction, muscle viscoelastic properties are changed. A general consensus seems to exist among muscle physiologists concerning the broad outlines of the contraction process. Nevertheless, the precise details are the subject of active investigation and debate.

Muscles exert force when activated by nerve stimulation or by artificial stimuli (electrode). When stimulated at a sufficiently high frequency, muscles can generate a maximal tension (tetanized muscle), which remains almost constant in time. The activity of the contracting mechanism is thought to be maximal. These stimuli start a chain reaction of chemical processes that initiate the actin filament and opposite myosin filament to build cross-bridge connection. The myofilaments, actin and myosin, are together the smallest functional unit of a muscle – the sarcomere (Fig. 2). This element generates

force in a muscle, and is often termed active element or contractile element in literature. Movement is initiated when the myofilaments slide past one another.

Muscle fiber consists of a large number of sarcomeres that are arranged in series. The alignment of sarcomeres in series observed in parallel arranged fibers attributes to the name of striated muscle. A large number of muscle fibers arranged in parallel form a muscle belly.

Muscle fibers are connected to bones *via* tendons which transfer the force generated in muscle, but also include additional compliance in musculature.

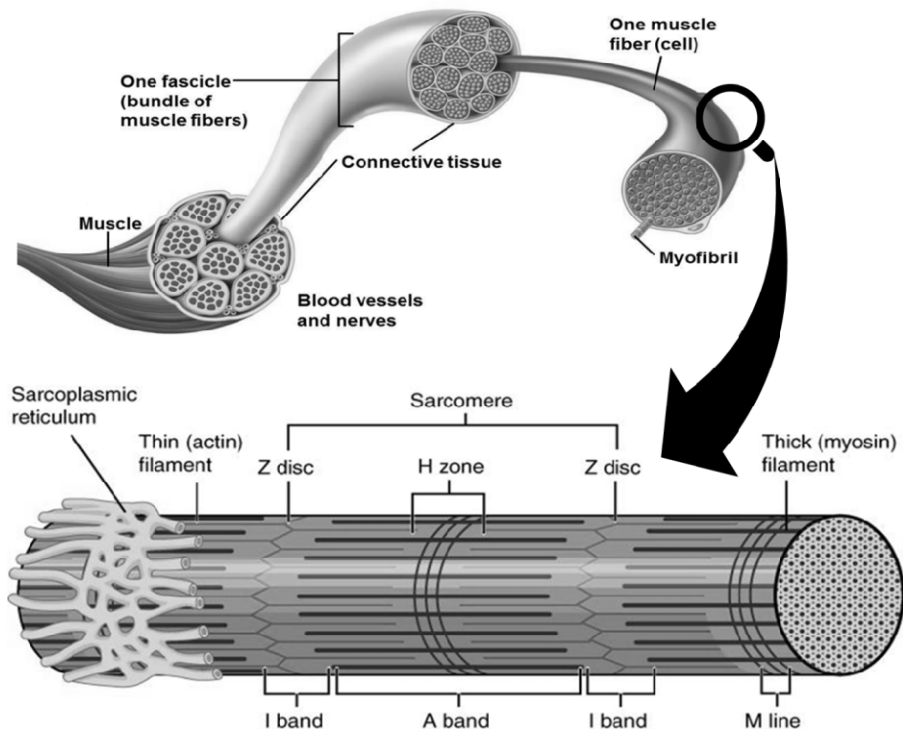


Fig. 2 – Scalable anatomy of a human muscle [image adopted from *Anatomy Corner – Image Resources for Students and Teachers*, <http://anatomycorner.com/>, accessed in November 2014].

The muscle force is produced by cross-bridges, while passive elements are tendons and connective tissue which covers and protect muscle fibers. Therefore this element is essential to be modelled correctly. The viscoelastic properties of the passive elements are also important for muscle behaviour and their role has to be taken into account for any reliable muscle models as it is shown in the following section.

3 Muscle models

A universal mathematical model of human muscle has not been developed yet. However, many authors have presented numerous models, each of them suitable for a very specific application. In this section, we will present Hill's and Huxley's models and our implementation of both models in computer simulations.

3.1 Hill's model

Hill was pioneer in muscle modelling [14] and numerous models rely on his muscle representation (Fig. 3). Winters and Stark [15] described Hill's macroscopic model as mechanical structure which contains: the Contractile Element (CE) – which generates force due to an activation signal, passive visco-elastic properties (originating from muscle force-length-velocity correlation); the Parallel Element (PE) – visco-elastic properties originating from connective tissues within a muscle unit such are epimysium, perimysium and endomysium; and the Series Element (SE) – to contribute for the tendon and aponeuroses. Muscle mass is presented through the inertial element with mass M . While a muscle generates force that shortens the muscle and therefore pull the link, the link and all other load pull the muscle representation with force F as denoted in Fig 3.

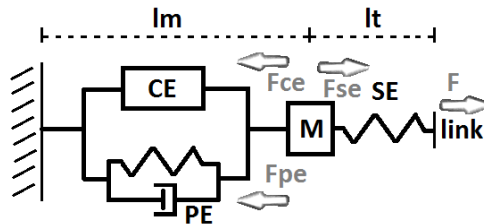


Fig. 3 – Muscle model representation according to Hill [15]. See text for details.

The force generation of CE depends on its velocity (v_m), on its length (l_m) and on its activation ($a(t)$)

$$F_{CE} = F_{max} a(t) f(l_m) g(v_m), \quad (1)$$

where: $f(l_m)$ – force-length relation of the muscle; $g(v_m)$ – force-velocity relation of the muscle; $a(t)$ – active state function (muscle activation) which belongs to the range $[0, 1]$. Note that all three components scale maximal isometric force at optimum muscle fiber length and zero velocity (F_{max}) in the range $[0, 1]$.

An expression for the extended force-velocity relation (where v_m is muscle shortening velocity and v_{max} denotes the dependence of the maximum velocity on the active state and length of the muscle) is given by (2):

$$g(v_m) = \frac{1 - v_m / v_{max}}{1 + 4v_m / v_{max}}. \quad (2)$$

The force, which contractile element delivers, depends on the contraction velocity and its length. The force that can be developed depends on the number of cross-bridges that can be formed, which is related to the amount of overlap of the actin and myosin filaments. The equation that describes the force-length relation according to Hill is given by (3), where: w – width of the force-length relationship; l_m – actual muscle length; l_{mopt} – optimum muscle length.

$$f(l_m) = 1 - \left(\frac{\left(\frac{l_m}{l_{mopt}} \right) - 1}{w} \right)^2. \quad (3)$$

The PE represents various connective tissues that run parallel to the muscle fibers and its visco-elastic properties are represented by spring and damper. According to Winters and Stark [15] the spring effect – F_p , of the PE can be described as partly exponential until PE stiffness reaches its max value and afterwards it behaves as linear spring (4). Parallel tissues have damping effect – F_d , as well F_d can be easily modelled by (5). The following labels are used: F_{max} – the force at which the element changes from exponential to linear elasticity; l_{mc} – the length at which the element changes from exponential to linear elasticity; l_m – actual muscle length; l_{ms} – slack muscle length; k_m, k_{ml} – spring constants; k_{ms} – shape parameter; B_m – the damping constant; v_m – the velocity of change of muscle length. The sum of F_p and F_d represents contribution of the PE:

$$F_p(l_m) = \begin{cases} 0, & l_m < l_{ms}, \\ \frac{k_{ml}}{k_{me}} \left(\exp(k_{me}(l_m - l_{ms})) - 1 \right), & l_{ms} \leq l_m \leq l_{mc}, \\ F_{mc} + k_m(l_m - l_{mc}), & l_m > l_{mc}. \end{cases} \quad (4)$$

$$F_d(v_m) = B_m v_m, \quad (5)$$

$$F_{pE} = F_p + F_d. \quad (6)$$

SE represents a tendon and transmits the force F_{SE} from muscle to the bone. Similarly to the spring effect of the PE it can be modelled partly as exponential and partly as linear spring where max tendon stiffness is obtained when the force transmitted through the tendon is F_{tc} which means at tendon length $l_t = l_{tc}$. Therefore, for F_{tc} – the force at tendon becomes linear; l_{ts} – the length at which tendon becomes linear; l_t – tendon length; l_{ts} – tendon slack length; k_t, k_{tl} – tendon spring constants; k_{te} – exponential shape parameter, it stands:

$$F_{SE}(l_t) = \begin{cases} 0, & l_t < l_{ts}, \\ \frac{k_{tl}}{k_{te}} \left(\exp(k_{te}(l_t - l_{ts})) - 1 \right), & l_{ts} \leq l_t \leq l_{tc}, \\ F_{tc} + k_t(l_t - l_{tc}), & l_t > l_{tc}. \end{cases} \quad (7)$$

3.2 Implemented Hill's model

Having in mind muscle representation shown in Fig. 3 and equations (1) – (7), one can derive full muscle model with tendon dynamics (8), while complete load from the rest of the body is represented by force F and therefore force F_{SE} . For our Hill's model implementation, we choose muscle length and velocity as state space variables: $\mathbf{X} = [x_1 \ x_2]^T = [l_m \ \dot{l}_m]^T$, while muscle activation a is an input and therefore a control parameter for the system.

$$\mathbf{X} = \begin{bmatrix} \dot{x}_1 \\ \dot{x}_2 \end{bmatrix} = \begin{bmatrix} x_2 \\ \frac{1}{M} [F - F_{CE}(x_1, x_2, a) - F_P(x_1) - F_d(x_2)] \end{bmatrix}. \quad (8)$$

Of special interest for muscle behaviour is stiffness of the overall muscle – tendon structure. During specific and repetitive tasks (e.g. walking), this stiffness can be exploited to decrease energy consumption. This overall muscle – tendon stiffness can be moderated for the same muscle – tendon length ($l_m + l_t = \text{const.}$) by muscle activity a so the passive elements of both PE and SE change their particular lengths l_m and l_t and accordingly their stiffness. For isometric condition, ratio l_m/l_t can be reduced in a case of higher muscle activity which leads to higher overall stiffness, but at the same time to the higher energy consumption which is correlated with muscle activity a .

3.3 Huxley's model

For more detailed insight into stiffness distribution one should use the most detailed model on microscopic level. Huxley was the first one to set the muscle model on this level [16], while Zahalak gave his contribution to enable numerical simulation on a microscopic level [17].

Huxley considered dynamics of the filaments within muscle and probability of establishing cross-bridges (connecting myosin heads to actin filaments inside sarcomeres). The distribution function $n(x, t)$ describes the distribution of attached cross-bridges, i.e. rate of connections between myosin heads and actin filaments, as a function of cross-bridge length x . The force dependence on velocity is implicitly included by assuming that cross-bridge attachment and detachment are time-dependent processes:

$$\frac{dn(x,t)}{dt} = a(t)f(x) \cdot \{\lambda(l) - n(x,t)\} - g(x)n(x,t), \quad (9)$$

where: $f(x)$ – probability of attaching myosin heads to actin filaments (probability of establishing cross-bridges); $g(x)$ – probability of detaching myosin heads from actin filaments (probability of breaking of established cross-bridges); $\lambda(l)$ – overlap factor depends on normalized muscle length $l = l_m/l_{mopt}$.

3.4 Huxley's model implementation

In order to apply the Distribution-Moment (DM) approximation, we assume that distribution function is Gaussian. Using the DM approximation from [17], we get system of three Ordinary Differential Equation (ODE) instead of Partial Differential Equation (PDE), as it is shown in [17]. If these assumptions are included into equation (9), i.e. (10) after integration. ζ is normalized sarcomere length with hypothesis that overall muscle length is sum of all sarcomere lengths in single muscle fiber while $\gamma = 0, 1, 2$:

$$\int_{\zeta} \zeta^\gamma \frac{dn(\zeta,t)}{dt} d\zeta = \int_{\zeta} \zeta^\gamma (a(t)f(\zeta)\{\lambda(l) - n(\zeta,t)\} - g(\zeta)n(\zeta,t)) d\zeta. \quad (10)$$

If Q_γ is defined by (11), three ODE for $\gamma = 0, 1, 2$ are obtained according to (12):

$$Q_\gamma(t) = \int_{-\infty}^{\infty} \zeta^\gamma n(\zeta,t) d\zeta, \quad (11)$$

$$\frac{dQ_\gamma(t)}{dt} + \gamma v(t)Q_{\gamma-1}(t) = \int_{\zeta} \zeta^\gamma (a(t)f(\zeta)\{\lambda(l) - n(\zeta,t)\} - g(\zeta)n(\zeta,t)) d\zeta. \quad (12)$$

Using DM approximation we get three state variables Q_γ . These variables representing the first three moments of the cross-bridge distribution function have direct physical meaning. The first distribution moment Q_0 represents the variable proportional to stiffness of the contractile tissue, the second one Q_1 is proportional to the total muscle force of contractile element and the third distribution moment Q_2 is proportional to the total elastic energy that exists in the cross bridge.

We implemented a generalized two-state muscle model of Huxley's type for calculating the force of contractile element in modified Hill's model. DM approximation is used to develop a system of ordinary differential equations (ODE) appropriate for numerical calculations and implementation in the simulation model.

Both models were implemented in Simulink Matlab (The Mathworks, Natick, USA).

4 Results of Comparative Analysis of Macroscopic Hill and Incorporated Huxley Cross-Bridge Muscle's Models

Following figures (Figs. 4 – 6) depict comparison between the system with muscles modeled after macroscopic Hill's theory and the system with incorporated Huxley's model and DM approximation. Since prime movers of the humans are skeletal muscles with their tendons, we use the similar setup for model validation: series elastic actuation containing muscle and tendon followed by inertial object replicating limb (Fig. 3). Simulation experiment exploits state space model presented by (8), while model parameters are listed in Appendix A.

Muscle contractile element force in cases of Hill's and Huxley's model when activated by single pulse activation is pointed out in Fig. 4. Fig. 4 demonstrates the core difference between the two models – generated force in contractile element (F_{CE}). One can see that more detailed Huxley approximation that considers establishment of cross-bridges within muscle units gives smoother shape of the muscle forces suggesting to be more suitable to the real muscle behaviour [18]. On the other hand, due its simplicity and computational efficiency Hill's model is acceptable for some purposes [19]. However, both representations give similar results on time and amplitude scales.

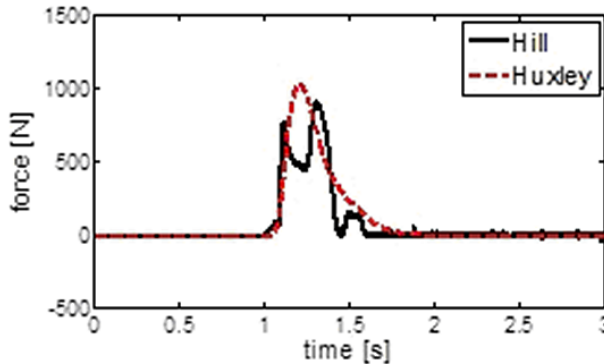


Fig. 4 – Muscle force in cases of macroscopic Hill and incorporated Huxley cross-bridge models as a result of computer simulation.

Due to different dynamics of generated force in active element of the muscle in cases of two models, as one can observe in Fig. 5, there is a slight difference in muscle lengths too. The muscle shortens due to single pulse neuro-activation, and the length change of this muscle in Hill's and Huxley's model is performed in the same way. Differences in muscle length are present especially during the transit process (observed length difference in Fig. 5 at 1.5 s), but those dissimilarities are acceptable and expected due to generated forces

presented above. The differences are smaller during stationary lengths: first and last second in Fig. 5.

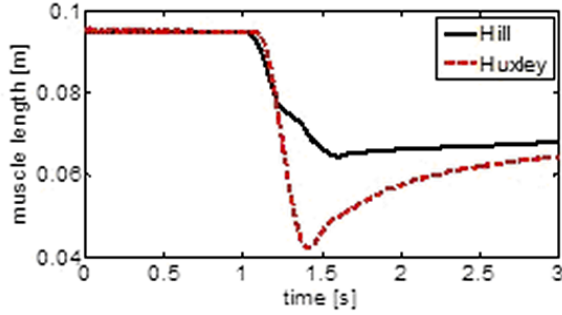


Fig. 5 – Muscle length in cases of macroscopic Hill's and incorporated Huxley's cross-bridge models as a result of computer simulations.

The results demonstrate smoother and more natural trajectories in case of incorporated Huxley's model compared to Hill's model. This might be caused by detailed approximation of physiological process inside the contractile element as force generator within muscle in Huxley's model. On the other hand, Huxley's model with its DM approximation requires more computational resources and it is therefore more time consuming. Contrarily, Hill's model gives less detailed approximation, but again accurate enough for some initial applications and more efficient/faster computational solution.

5 Model Based Analysis of Energy Distribution in Muscle-Tendon Structure

Human walking or running are prime examples of exploiting dynamic properties of muscle-tendon structure. Therefore, storage of strain energy, as well as its recovery, is unidirectional way towards copying biomimetic principles for technical solutions [19, 20]. To fully understand and exploit phenomenon and muscle physiology, we do need to distinguish between elasticity in muscle and tendon. Many authors have already discussed energy distribution between a muscle and its tendon [21, 22]. This is also confirmed by numbers of simulation experiment in our research. Energy, which could be recovered, is energy stored in purely elastic components: tendon (SE) – E_{pt} , and muscle passive element (PE) – E_{pm} .

$$E_{pt}(l_t, \Delta l_t) = \int_{l_t}^{l_t + \Delta l_t} F_{SE}(x) dx = \int_{l_t}^{l_t + \Delta l_t} k_{SE}(x) x dx, \quad (13)$$

$$E_{pm}(l_m, \Delta l_m) = \int_{l_m}^{l_m + \Delta l_m} F_p(x) dx = \int_{l_m}^{l_m + \Delta l_m} k_p(x) x dx. \quad (14)$$

The aim of this simulation experiment is to point out role of tendon compliance. Namely it is well known that during walking, cycling, or similar repetitive tasks, as well as while sudden unexpected disturbances tendon is the one who absorbs impact and later one recover energy in order to save muscle endurance [23 – 24]. We examined three cases in simulations. We assumed passive muscle (muscle activity is supposed to be zero $a = 0$) distributed by sinusoidal external force F (see Fig. 3) of the same magnitude 150 N and two difference frequencies: 10 Hz and 100 Hz.

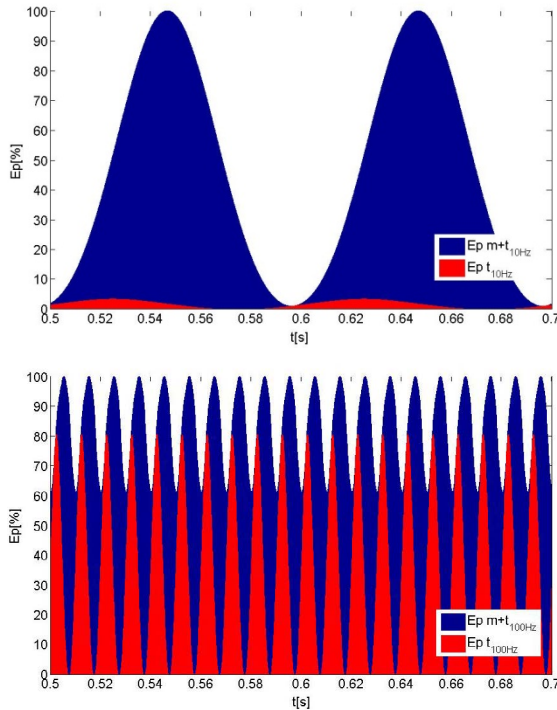


Fig. 6 – Distribution of stored strain energy between muscle and tendon stretched by periodic external force of different frequencies – 10 Hz (up), 100 Hz (down).

Results of energy store-and-release in muscle and tendon are presented in Fig. 6 for time interval of 0.2 s. Strain energy stored in the tendon is depicted in red, while total strain energy (strain energy stored in tendon plus strain energy stored in muscle) is given in blue.

One can notice that force impact initially influence tendon extension (and therefore energy storage in the element). Furthermore, fast disturbances affect muscle itself less, i.e. the tendon absorbs most of the energy delivered to the system. Therefore, muscle endurance is saved. Otherwise, strain energy stored

in muscle prevails. From the analysis an importance conclusion for repetitive and cyclic task such is cycling, running, or hopping can be drawn: The higher frequency of a movement is, elastic energy stored and released in muscles in each cycle is less and therefore length of the muscles do not change that rapidly, or in other words tendon save muscle endurance.

6 Discussion and Conclusions

The paper elaborated utilization of different muscle models for comprehensive understanding and accurate prediction of biological systems behavior. Although some preliminary conclusion can be drawn about potential use of Hill's and Huxley's muscle models, there are still numerous opened questions:

- 1) How to estimate full set of necessary model's parameters for different muscles?
- 2) How to perform model validation, since it is necessary for wider class of muscle velocities and external forces?
- 3) Which Electromyography (EMG) representation fits best input of the model?
- 4) How to rate comparison between measured and simulation results?

Further prospective of the model is expected through the stiffness estimation which is one of the key features for safe interaction between humans and human-like services, compliance control of human-like actuation, exploitation of human patterns in control of human-like actuators, and optimization techniques for activation of the artificial muscles. Since accurate control of contemporary robots rely solidly on its dynamics and compensate for well modeled components of it, why this study would not be direction in control of novel human-like actuated service robots?

Since biologically-inspired solutions are getting more common in the technical world, the ongoing research is overall expected to be exploited in numerous directions for better understanding of physiology itself.

7 Acknowledgement

The work on this project was partly supported by the Ministry of education, science, and technological development, Republic of Serbia, grant No. TR35003, and partly by the Ministry of education, science, and technological development, Republic of Serbia, grant No. OS175016.

Authors would like to thank prof. Veljko Potkonjak, and prof. Mirjana B. Popović from University of Belgrade – School of Electrical Engineering for their valuable advices during the work on this paper.

8 Appendix A

Table 1
Muscle and tendon model parameters [25 – 29].

| Parameter | Label | value |
|---------------------------------------|-------------|--------------|
| muscle mass | M_m | 0.95 [kg] |
| max isometric muscle force | F_{\max} | 3913 [N] |
| optimal fiber length | $l_{m,opt}$ | 0.0959 [m] |
| maximal unloaded shortening velocity | V_{\max} | 0.5179 [m/s] |
| activation time constant | t_{act} | 0.0012 [s] |
| deactivation time constant | t_{deact} | 0.012 [s] |
| width of force-length curve | W | 0.643 |
| exponential shape parameter | k_{te} | 3022 [1/m] |
| tendon spring constant | k_{tl} | 31140 [N/m] |
| tendon spring constant | k_t | 635540 [N/m] |
| tendon slack length | l_{ts} | 0.3185 [m] |
| length at which tendon becomes linear | l_{tc} | 0.3185 [m] |
| force at which tendon becomes linear | F_{tc} | 200 [N] |
| exponential shape parameter | k_{me} | 90.4 [1/m] |
| parallel spring constant | k_{ml} | 487.5 [N/m] |
| parallel spring constant | k_m | 6770 [N/m] |
| passive muscle slack length | l_{ms} | 0.0959 [m] |
| length at which spring becomes linear | l_{mc} | 0.125 [m] |
| force at which spring becomes linear | F_{mc} | 69.4723 [N] |
| parallel damping constant | B_m | 257.1 [Ns/m] |

7 References

- [1] V. Potkonjak, B. Svetozarevic, K. Jovanovic, O. Holland: The Puller-Follower Control of Compliant and Noncompliant Antagonistic Tendon Drives in Robotic System, *International Journal of Advanced Robotic Systems*, Vol. 8, No. 5, 2012, pp. 143 – 155.
- [2] K. Jovanovic, V. Potkonjak, O. Holland: Dynamic Modelling of an Anthropomorphic Robot in Contact Tasks, *Advanced Robotics*, Vol. 28, No. 11, 2014, pp. 793 – 806.
- [3] F. Daerden, D. Lefeber: Pneumatic artificial muscles: actuators for robotics and automation, *European Journal of Mechanical and Environmental Engineering*, Vol. 47, No.1, 2002, pp. 10 – 21.

- [4] T.W. Secord: Design and application of a cellular, piezoelectric, artificial muscle actuator for biorobotic systems, PhD thesis, Dept. of Mechanical Engineering, Massachusetts Institute of Technology, Boston, Massachusetts, USA, 2010.
- [5] Y. Bar-Cohen: Electroactive Polymer (EAP) Actuators as Artificial Muscles: Reality, Potential, and Challenges, 2nd ed., SPIE Press, Vol. PM136, 2004.
- [6] H. Taniguchi: Flexible Artificial Muscle Actuator Using Coiled Shape Memory Alloy Wires, Proc. the 3rd International Conference on Biomedical Engineering and Technology- ICBET, Copenhagen, Denmark, Vol. 7, May 2013, pp. 54 – 59.
- [7] I. W. Hunter, S. Lafontaine: A comparison of muscle with artificial actuators, IEEE Solid-State Sensor and Actuator Workshop, Hilton Head Island, SC, USA, Jun 1992, pp.178 – 185.
- [8] D. Schneck: Mechanics of Muscle, 2nd ed., New York University Press, New York, 1992.
- [9] M. Latash: Neurophysiological basis of movement, Champaign, Illinois, USA: Human Kinetics, 1998.
- [10] Y. Ariga, D. Maeda, H. Pham, M. Uemura, H. Hirai, F. Miyazaki: Novel Equilibrium-Point Control of Agonist-Antagonist System with Pneumatic Artificial Muscles, IEEE International Conference on Robotics and Automation, Minnesota (ICRA2012), USA, 2012, pp. 1470 – 1759.
- [11] M. Grebenstein, P. Van der Smagt: Antagonism for a Highly Anthropomorphic Hand-Arm System, Advanced Robotics, Vol. 22, No. 1, 2008, pp. 39 – 55.
- [12] Y. Nakanishi, S. Ohta, T. Shirai, Y. Asano, T. Kozuki, Y. Kakehashi, H. Mizoguchi, T. Kurotobi, Y. Motegi, K. Sasabuchi, J. Urata, K. Okada, I. Mizuuchi, M. Inaba: Design Approach of Biologically-Inspired Musculoskeletal Humanoids, International Journal of Advanced Robotics Systems, Vol. 10, 2013, pp. 1 – 13.
- [13] S. Wittmeier, C. Alessandro, N. Bascarevic, K. Dalamagkidis, A. Diamond, M. Jeantsch, K. Jovanovic, R. Knight, H.G. Marques, P. Milosavljevic, B. Svetozarevic, V. Potkonjak, R. Pfeifer, A. Knoll, O. Holland: Toward Anthropomorphic Robotics: Development, Simulation, and Control of a Musculoskeletal Torso, Artificial Life, Vol. 19, No. 1, 2013, pp. 171 – 193.
- [14] A. Hill: The Heat of Shortening and the Dynamic Constant of Muscle, Proc. of the Royal Society of London - Series B: Biological Sciences, Vol. 126, No. 843, 1938, pp. 136 – 195.
- [15] J. M. Winters, L. Stark: Muscle Models: What is Gained and What is Lost by Varying Model Complexity, Biological Cybernetic, Vol. 55, No.6, 1987, pp. 403 – 420.
- [16] A. F. Huxley: Muscle Structure and Theories of Contraction, Progress in Biophysics and Biophysics Chemistry, Vol. 7, 1958, pp. 257 – 318.
- [17] G. I. Zahalak: A Distribution-Moment Approximation for Kinetic Theories of Muscular Contraction, Mathematical Biosciences, Vol. 55, No. 1–2, 1981, pp. 89 – 114.
- [18] S. Đorđević, S. Tomažić, M. Narici, R. Pišot, A. Meglič: In-Vivo Measurement of Muscle Tension: Dynamic Properties of the MC Sensor During Isometric Muscle Contraction, Sensors, Vol. 14, No.9, 2014, pp. 17848 – 17863.
- [19] J. Denoth: The Dynamics of Hill's Muscle Model-Considerations and Applications, Biomechanics: Current Interdisciplinary Research Developments in Biomechanics, Vol. 2, 1985, pp. 617– 622.
- [20] F. Bauer, A. Fidlin, W. Seemann: Energy Efficient Bipedal Robots Walking in Resonance, ZAMM - Journal of Applied Mathematics and Mechanics, Vol. 94, No. 11, 2014, pp. 968 – 973.

Hill's and Huxley's Muscle Models – Tools for Simulations in Biomechanics

- [21] M. Reis, F. Iida: An Energy Efficient Hopping Robot Based on Free Vibration of a Curved Beam, *IEEE/ASME Transactions on Mechatronics*, Vol. 19, No. 1, 2013, pp. 300 – 311.
- [22] P. M. H. Rack, H. F. Ross, A. F. Thilmann, D. K. W. Walters: Reflex Responses at the Human Ankle: The Importance of Tendon Compliance, *Journal of Physiology*, Vol. 344, 1983, pp. 503 – 524.
- [23] A. Biewener: Muscle-tendon stresses and elastic energy storage during locomotion in the horse, *Comparative Biochemistry and Physiology Part B: Biochemistry and Molecular Biology*, Vol. 120(1), 1998, pp. 73 – 87.
- [24] H. C. Astley, T. J. Roberts: Evidence for a Vertebrate Catapult: Elastic Energy Storage in the Plantaris Tendon During frog Jumping, *Biology letters – Biomechanics*, Vol. 8, No. 3, 2012, pp. 386 – 389.
- [25] M. L. Audu, D. T. Davy: The Influence of Muscle Model Complexity in Musculoskeletal Motion Modeling, *Journal of Biomechanical Engineering*, Vol. 107, No.2, 1985, pp. 147 – 157.
- [26] D. Schneck: *Mechanics of Muscle*, 2nd edition, New York University Press, New York, USA, 1992.
- [27] J. M. Winters, L. Stark: Estimated Mechanical Properties of Synergistic Muscle Involved in a Variety of Human Joints, *Journal of Biomechanics*, Vol. 21, No. 12, 1988, pp. 1027 – 1041.
- [28] G. Yamaguchi: *Performing Whole Body Simulation of Gait with 3D Dynamic Muskuloskeletal Models, Multiple Muscle Systems: Miomechanics and Movement Organization*, Springer – Verlag, New York, 1990.
- [29] A. N. Vardy: Parameter Estimation of the Huxley Cross-Bridge Model in Humans, *IEEE Annual International Conference on Engineering and Biology Society (EMBC)*, Aug. 28 – Sept. 1, 2012, San Diego, CA, USA, pp. 4827 – 4830.